INVESTIGATION OF ABNORMAL SEEPAGES IN AN EARTH DAM USING RESISTIVITY TOMOGRAPHY

Chih-Ping Lin [1], Yin-Chun Hung [2], Zen-Hung Yu [3], and Po-Lin Wu [4]

ABSTRACT

This study was aimed at assessing the performance of electrical resistivity tomography (ERT) applied to the investigation of seepage in earth dams through a case study. Several abnormal leaks appeared on the downstream face of an earth dam after the dam was reconstructed to raise the maximum reservoir water level. A study was conducted to investigate the mechanism of the abnormal leakage with the assistance of ERT. Three two-dimensional (2D) ERT survey lines were deployed on the left abutments, dam crest, and downstream shell, respectively. Periodic measurements were additionally collected on the downstream shell for time-lapse measurements. To gain confidence and avoid over interpretation, the results of 2D ERT were appraised by forward modeling and synthetic inversion. Combining ERT results with geotechnical monitoring data clearly indicates the likely mechanism of abnormal seepage. Time-lapse measurements further support the inducted mechanism. Integration of ERT exploration with time-lapse ERT measurements and geotechnical monitoring data was demonstrated to better understand the possible mechanism of the abnormal seepage.

Key words: Electrical resistivity tomography (ERT), seepage, leakage, earth dam.

1. INTRODUCTION

In Taiwan, more than 75% of reservoirs are earth dams. The most common problem in earth dams is abnormal seepage or excessive leakage. Normal seepage through the earth dam body is a planned and accepted process, and it is typically drained by designed zoned filters. However, anomalous seepage may occur sometimes by developing preferential flow paths in the dam body (Lee *et al*. 2005). Thoughtless treatment of an abnormal seepage may result in piping in the dam that may eventually cause dam failure (Malkawi and Al-Sheriadeh 2000). Therefore, seepage in an earth dam should be well controlled to maintain the dam's stability.

Typical dam safety surveillance mainly utilizes visual inspections supported by limited instrumentation. However, visual inspections do not provide information inside the dam, while monitoring instrument provides engineering parameters only at discrete points with limited spatial coverage of the dam (Lin *et al*. 2005). There is a growing demand for the use of non-intrusive geophysical techniques to "see" into the dam and facilitate early detection or diagnosis of anomalous phenomena (Voronkov *et al*. 2004). Electrical resistivity tomography (ERT) and self potential method have been increasingly applied for seepage investigations and dam status control (Abuzeid 1994; Okko *et al*. 1994; Panthulu *et al*. 2001; Karastathis *et al*. 2002; Turkmen *et al*. 2002; Oh *et al*. 2003; Lim *et al*. 2004; Sjödahl *et al*. 2005; Song *et al*. 2005; Cho and Yeom 2007; Kim *et al*. 2007). The change in soil moisture content accompanies the abnormal seepage. Under a given geological condition, ground resistivity is sensitive to variation of hydrophysical property. The ERT provides 2D or even 3D subsurface resistivity visualization. Time-lapse measurements can further enhance its capability to detect seepage anomalies (Johansson and Dahlin 1996; Sjödahl *et al*. 2010). Hence, it seems natural to choose ERT as one of the major geophysical methods for assisting diagnosis of leakage problem. Resistivity anomalies may progress to a significant extent and be detected by ERT. However, often what these anomalies represent and their implications are not clear. Most case studies showed the testing results to qualitatively support what had been known or come up with a speculation without in-depth examination or verification. Although significant progress has been made, the method is still not completely adapted for standard industrial practice. Furthermore, dams often presents difficult site conditions for ERT surveys and their geometry associated with the topography and zoned material property can be a complicating factor in the evaluation process (Sjödahl *et al*. 2006; Kim *et al*. 2007).

This paper introduces a case study to demonstrate the use of ERT and assess the performance of ERT in the investigation of abnormal seepage at the Hsin-Shan earth dam, Taiwan. Several abnormal leaks appeared on the downstream face after the dam was reconstructed to raise the maximum reservoir water level. A study was conducted to investigate the mechanism of the abnormal leakage with the assistance of electrical resistivity tomography (ERT). The importance of time-lapse measurements and integration with geotechnical monitoring data is emphasized. To gain confidence and avoid over interpretation, 2D ERT were appraised by forward modeling and synthetic inversion. Integration of ERT exploration with time-lapse ERT measurements and geotechnical monitoring data was demonstrated to better understand the possible mechanism of the abnormal seepage.

Manuscript received May 10, 2013; revised July 31, 2013; accepted July 31, 2013.

[1] Professor (corresponding author), Department of Civil Engineering, National Chiao Tung University, Hsinchu, Taiwan (e-mail: cplin@mail.nctu.edu.tw).

[2] Ph.D. candidate, National Chiao Tung University, Hsinchu, Taiwan.

[3] Engineer, Institute of Planning & Hydraulic Research, Water Resources Agency, Taiwan.

[4] Post doctorate, National Chiao Tung University, Hsinchu, Taiwan.

2. ERT BACKGROUND

In the resistivity method an electrical current is introduced into the ground and the resulting potential distribution is measured. Typically one pair of steel electrodes is used to inject current and another pair is used to measure potentials. The Wenner array where electrodes are equally spaced with two out current electrodes and two inner potential electrodes is illustrated in Fig. 1(a). If the subsurface resistivity distribution is homogeneous, the resistivity can be determined as

$$\rho_a = K\frac{V}{I} \tag{1}$$

where V is the voltage between the two potential electrodes, I is the current, K is the geometric factor (*e.g.*, $K = 2\pi\ a$ for Wenner array), and ρ_a is the measured resistivity. In practice this is never the case, the resistivity determined by Eq. (1), ρ_a, is termed apparent resistivity, which can be thought of as a weighted mean value of the conductivities of all current paths between the potential electrodes. From such a measurement, information about the average electrical resistivity of specific subsurface volume is received. By altering the distances between the electrodes, different volumes of the subsurface are sensed and additional information about resistivities at different depths is obtained. Various four-electrode array configurations for are available, such as Wenner, Schlumberger, dipole-dipole, pole-dipole, pole-pole, and gradient arrays.

The resistivity method has evolved from 1D to 2D and ultimately 3D measurements. The 1D vertical electrical sounding, VES, uses the same midpoint for a specific electrode configuration. By systematically increasing the electrode separation, the current is forced deeper into the subsurface and the result is the apparent resistivity at increasing depths for a given location. The relationship between electrode spacing and apparent resistivity is used to back calculate the resistivity profile assuming subsurface is a horizontally-layered medium. Geological features are typically more complex than a horizontally-layered medium. By varying the midpoint of the series of VES measurements, it results in an extended 2D collection of measurements at different depths along a line. Taking the Wenner array for example, Fig. 1(b) illustrates the sequence of data collection and construction of a pseudosection. The resulting data represents a 2D pseudo section of the subsurface beneath the electrode line (Griffiths *et al*. 1990). The inversion of the 2D survey data results in a resistivity cross section along the electrode line, and is known as the 2D electrical resistivity tomography (2D ERT). The combination of separately measured 2D survey lines in parallel, and interpreted (inverted) in 3D, or 3D surveys based on 3D arrays with cross-line measurements, 3D surveying, is developing rapidly and its used has become more common recently (Bentley and Gharibi 2004). Although 3D ERT is now available and is not restricted by the 2D assumption, field conditions often obstruct 3D surveys. In geological investigation, 2D ERT remains to be the state of the practice due to its simplicity in field works and less space requirement.

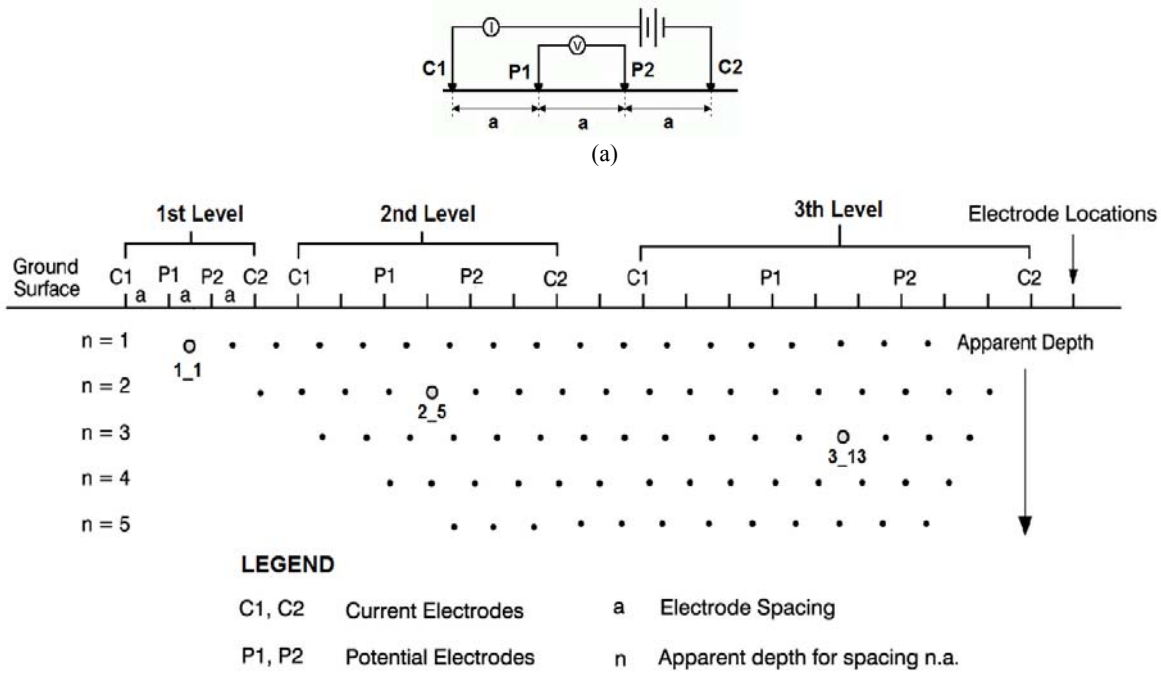

Fig. 1 (a) Four-electrode Wenner Array; (b) Sequence of data collection and construction of a pseudosection for 2D ERT

3. SITE DESCRIPTION

Hsin-Shan reservoir is located on a branch of Keelung River in the northern part of Taiwan (Fig. 2(a)). It is an off-channel reservoir with storage diverted from the Keelung River. The reservoir stores river water during rainy periods in typical wet winters and during typhoon storms in the summer. The summer is considered as a relative low precipitation season. The dam was first constructed in 1980. To meet the increasing demand for water supply, the dam crest was raised from EL. 75 m to EL. 90 m in 1998, and the designed storage of the reservoir was increased from 4×10^6 m^3 to 10×10^6 m^3, accordingly.

The major cross section of the dam is shown in Fig. 3. The original dam was constructed up to EL. 75 m as a zoned earth dam with inclined core and toe drain. To raise the dam while accommodating the original dam configuration, the added core was further inclined toward the downstream and a vertical drain of unusual shape was added. Not long after the water level was raised above the old crest elevation, a few abnormal seepage spots were identified on the surface of the downstream slope, as shown in Fig. 4. The water level was decided to remain below EL. 83 m before the abnormal seepage problem is clarified.

The rocks at the site are mainly composed of medium to coarse massive sandstones with slight calcareous inclusions. These sedimentary strata dip into the reservoir on the left bank, and serve as scarp slopes in the right bank of the reservoir, as shown in Fig. 2(b). Both dam abutments are located on the hard massive sandstone, but sets of joints and the alternating weak layers can be observed in the dam area (CGS 1998). The abnormal seepage was attributed to the poor geological condition of the left abutment in earlier field investigations (TWC 2001). But the right abutment is by no means more water resistant than the left abutment according to the geological section and construction record. In fact a curtain grout was installed in 1988 at the right abutment when the dam was first constructed. Another set of curtain grouts on both sides of abutment was installed in 1999 before the dam was further raised, as shown in Fig. 2(a). Regardless of the effort, abnormal seepage was found on the surface of the downstream slope when the water level was raised above the old dam crest (EL. 75). The abnormal seepage appeared to be more prominent towards the left abutment and the remediation called for another curtain grout at the left abutment, which was completed in 2002 as shown in Fig. 2(a). But abnormal seepage phenomenon remains unchanged and leaves the remediation work in vain. The administrator of the dam preferred not to utilize destructive investigation methods and called upon non- intrusive geophysical techniques to investigate the mechanism of the abnormal seepage.

4. FIELD ACQUISITION AND DATA ANALYSIS

The earth dam is covered by 3 m of ripraps except for the crest and a downstream passageway, making extensive self potential survey and transverse ERT survey lines on the shell difficult. As a first attempt of geophysical investigation on the Hsin-Shan earth dam, three survey lines were deployed as shown in Fig. 4. To see into the earth dam, Line A extends the whole range of the crest while Line B covers the straight part of the downstream passageway. Line C is located at the left abutment and passes through the curtain grout. Line B was further used for long term monitoring to investigate the relationship between resistivity variation and other environmental factors.

The Syscal Pro Switch48 resistivity meter (manufactured by IRIS instruments), which combines a transmitter, a receiver and a switching unit in one single casing, was used for the field resistivity measurements. Stainless steel electrodes (30 cm long and 1.0 cm in diameter) were used to set up the electrode array in the field. The recorded apparent resistivity data were processed using the Res2Dinv (Geotomo Software 2007). Various array configurations for 2D electrical imaging surveys are available, such as Wenner, Schlumberger, dipole-dipole, pole-dipole, and pole-pole arrays. It is generally recognized that the Wenner arrays are less sensitive to noise and have high vertical resolution, while dipole-dipole arrays have lower signal-to-noise ratios but have better lateral resolution (Dahlin and Zhou 2004). Repeated measurements were to be conducted on Line B to investigate the relationship between resistivity variation and other environmental factors. A preliminary test utilizing dipole-dipole (Fig. 5(a)), Wenner (Fig. 5(b)), pole-dipole (Fig. 5(c)), and pole-pole (Fig. 5(d)) arrays was conducted to evaluate their repeatability. The results are shown in Fig. 5. The Wenner array showing the best repeatability was used for subsequent investigations, particularly for the time-lapse measurements on Line B.

The absolute value of resistivity may not directly reflect hydrophysical property since it is also affected by the type of soil or rock. The investigation of abnormal seepage may be complemented by studying the changes of the subsurface resistivity with time. Time-lapse resistivity imaging has been successfully applied in monitoring water infiltration of unsaturated zone (Barker and Moore 1998), fluctuation of groundwater level, and salt water intrusion (Dahlin and Leroux 2006). In a more similar context, Johansson and Dahlin 1996 and Sjödahl *et al.* 2006 utilized time-lapse ERT to monitor seepage in earth embankments. To do so, two-dimensional resistivity imaging surveys were repeated over the same line at the downstream slope (Line B) on a monthly basis. Since a pure comparison of individual inversion results often suffers from differently constructed inversion artifacts or blurs, the time-lapse inversion was used to focus on the changes in the subsurface resistivity with time. In time-lapse inversion, a smoothness constraint is applied not only to the spatial variation but also to the temporal variation between the data sets (Loke 2001).

5. RESULTS AND DISCUSSION

5.1 Results of ERT Surveys

Special attention was paid to the left abutment in earlier investigations. Thus two curtain grouts had successively installed to reduce the leakage. The result of ERT at line C passing through the curtain grout is first examined to evaluate the effectiveness of grouting at the left abutment. The inverted resistivity cross-section is shown in Fig. 6. An apparent low resistivity zone can be seen from Distance 20 m to 70 m near EL. 80 m. This is attributed to the 3D effect of a nearby water intake steel pipe running through. Line C intersects with the curtain grouts at Distance 100 m. But the survey line is not perpendicular to the curtain grouts as shown in Fig. 4. A vertical band of high resistivity exists from Distance 60 m to 100 m. This is believed to be the 3D effect mapping of the solidified ground by the grouting. No apparent lateral flaw in terms of low resistivity zone is found in the grouting area and at the downstream side of the curtain grout.

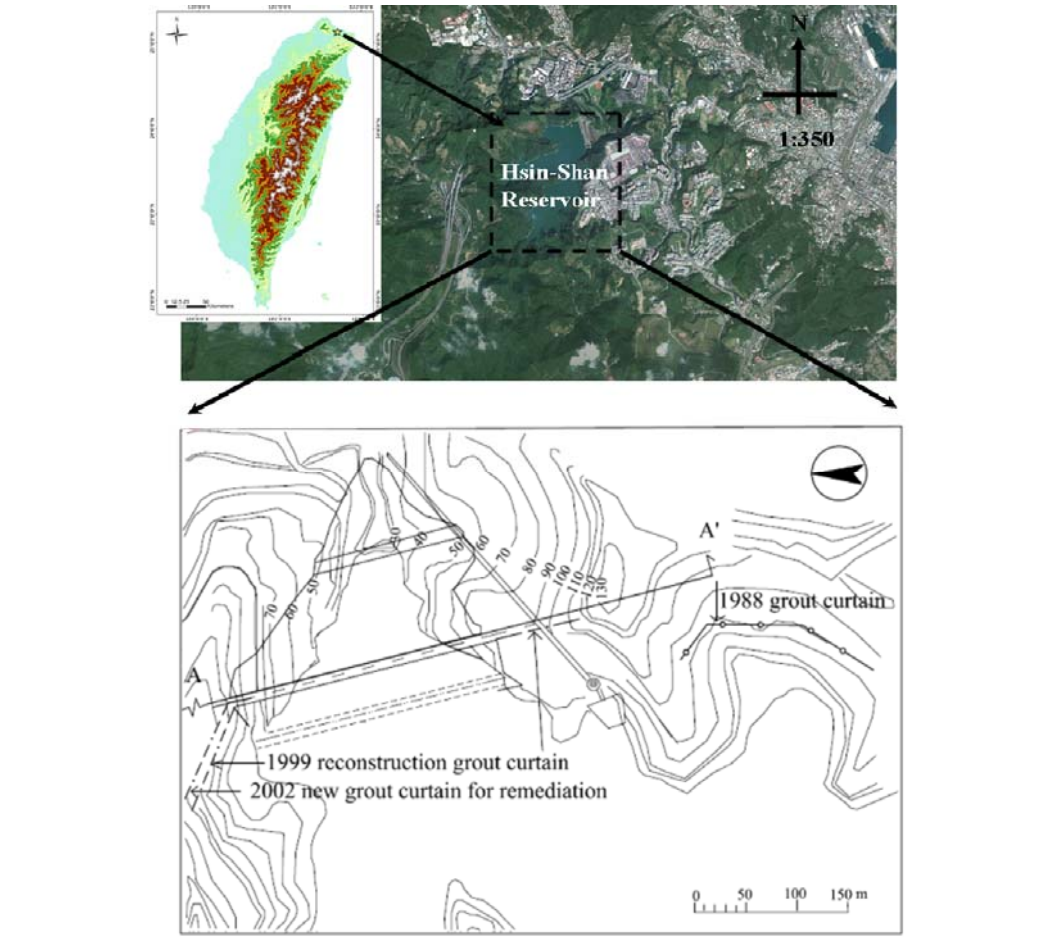

Fig. 2 (a) Geographical and (b) geological illustration of the study area

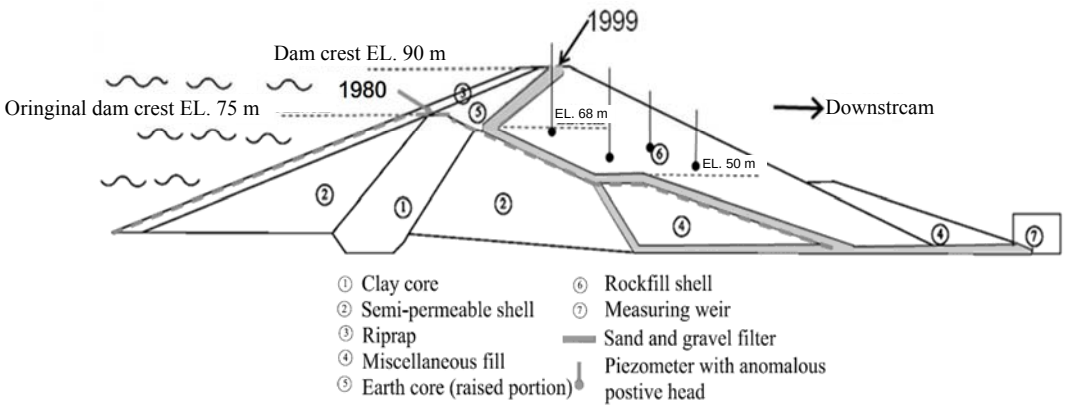

Fig. 3 Major cross-section of the Hsin-Shan zoned earth dam

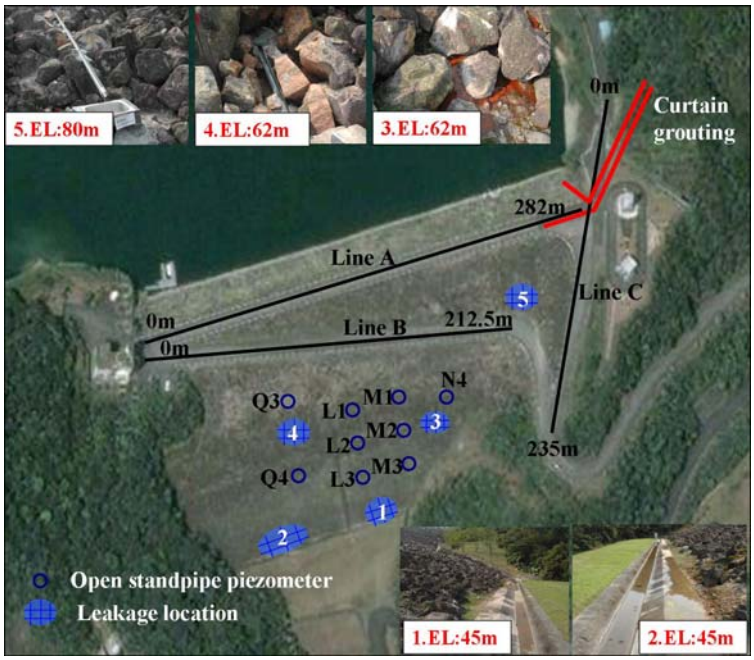

Fig. 4 Layout of ERT survey lines and photographs showing abnormal seepages at the downstream face

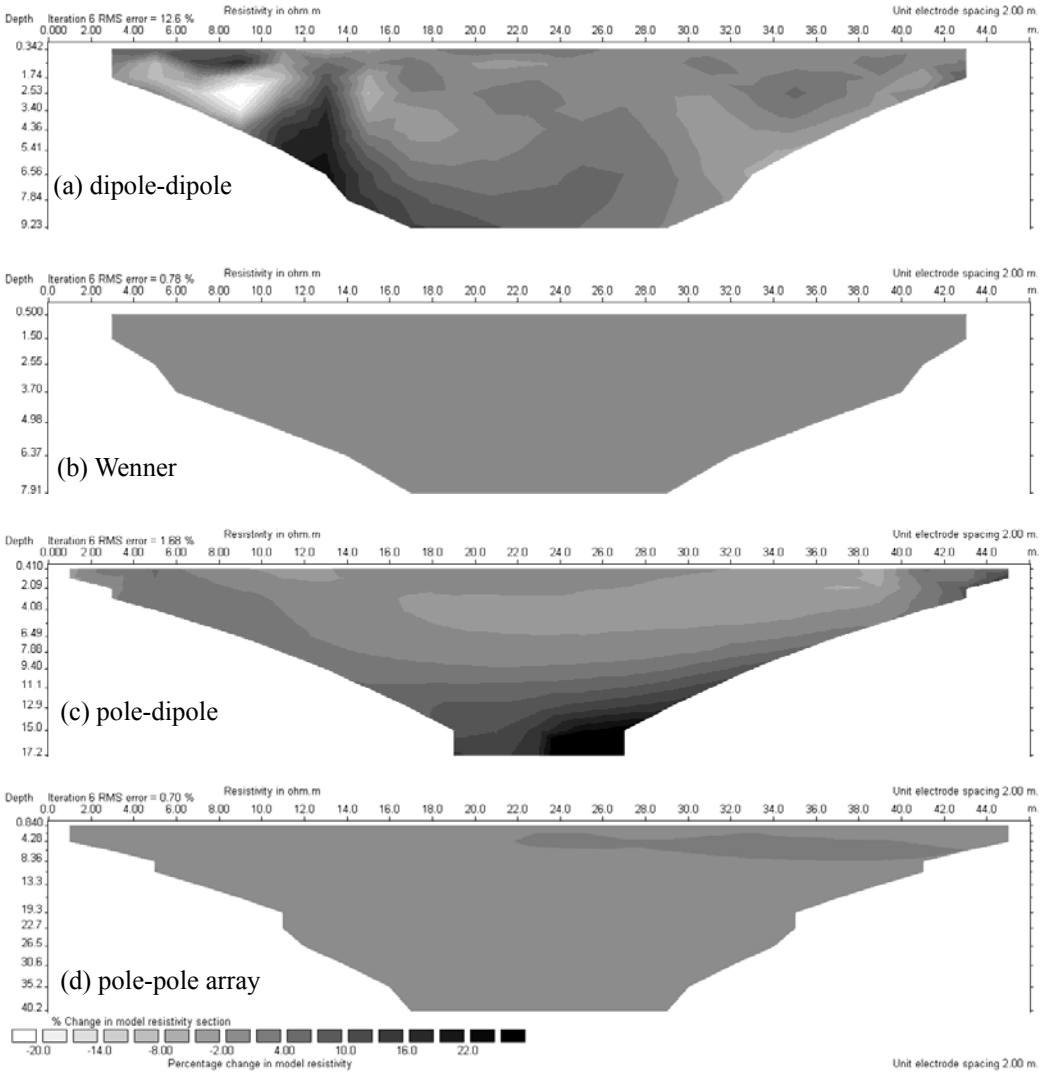

Fig. 5 Percentage change of inverted resistivity between two repeated measurements for (a) dipole-dipole; (b) Wenner; (c) pole-dipole; and (d) pole-pole array, respectively

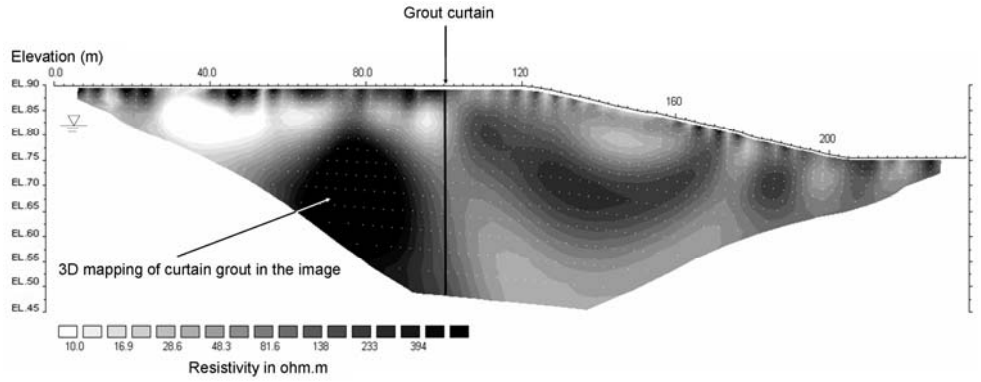

Fig. 6 Inverted resistivity cross-section for Line C at the left abutment

The inverted resistivity cross-section from Wenner array along the dam crest is shown in Fig. 7. A relative low resistivity layer is located near and above the reservoir level. In particular, two low resistivity zones are identified. One is located at Distance 30 ~ 60 m and EL. 79 ~ 84 m, which is mostly above the reservoir level. The other is located at Distance 200 ~ 250 m and EL. 76 ~ 84 m. Since most area of this low resistivity layer is located above the reservoir level, it may be attributed to wetted area or perched groundwater due to rainfall infiltration. Another deeper zone of low resistivity can be found at Distance 70 ~ 100 m below EL. 61 m. It should be noted that this low resistivity zone is mostly below the drainage layer. It is also below the elevation of the abnormal seepage.

Figure 8 presents the inverted resistivity cross-section of Line B on the downstream shell. The result shows lower resistivity at elevation above EL. 60 m. Two low resistivity anomalies are located at Distance 68 ~ 90 m and 150 ~ 180 m, respectively at elevation EL. 68 ~ 75 m and 60 ~ 73 m. Three ground-water observation wells are located near the downstream side of Line B, as shown in Fig. 4. The well water levels are projected on the resistivity image in Fig. 8. The two low resistivity zones seem to be well above the seepage phreatic line, suggesting two perched wet areas in the downstream shell.

5.2 Qualitative Appraisal

The resistivity models (or images) obtained by ERT reveal some interesting phenomena. However, geophysical inverse problems are inherently ill-posed. The model we would like to image is an infinite-dimensional space that is parameterized in terms of cells of finite area or volume, but we are limited by sparse sampling of the data space with noises. Questions often arise as to what features are resolvable in the ERT image? What parts of the model can we believe in terms of the scale of structure? To answer these questions some sort of appraisal analysis must be carried out with the model obtained from the inversion. Several appraisal quantities have been proposed such as model resolution matrix, cumulate sensitivity matrix, and depth of investigation index (Oldenburg and Li 1999; Friedel 2003; Nguyen *et. al*. 2009; Oldenborger and Routh 2009). For a non- linear inverse problem, these appraisal analyses are primarily carried out in a linearized sense about the final model at the convergence. The results of these advanced appraisal analysis are difficult to visualize and interpret. A built-in option in the Geotomo Res2Dinv software (Geotomo Software 2007) used is to display the model blocks sensitivity, as shown in Fig. 9 for Line B (before topography correction). Those blocks below the low resistivity zones and at the sides of the model show lower sensitivities. However, the sensitivity map does not provide engineers intuitive information as to how the inverted resistivity image could possibly deviate from the actual resistivity distribution.

The earth dam is a man-made structure. It is possible to construct a resistivity model based on the inverted resistivity cross-section and educated guess. A simplified resistivity model for Line B before topography correction is shown in Fig. 10(a). Due to water infiltration, the top layer is relatively low in resistivity underlain by three gradually higher resistivity layers. Two low resistivity zones are included near the bottom of the top layer to simulate the wetted areas. A forward model was performed using Res2Dmod (Geotomo Software 2002) to generate synthetic data

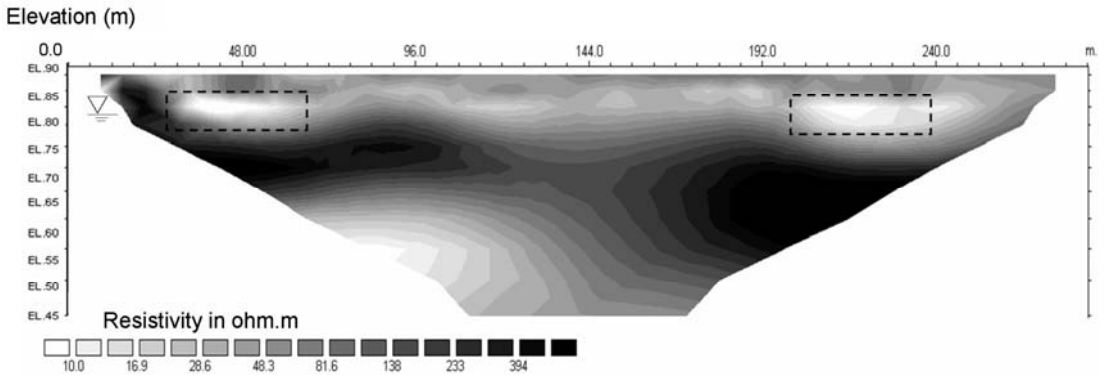

Fig. 7 Inverted resistivity cross-section for Line A along the dam crest

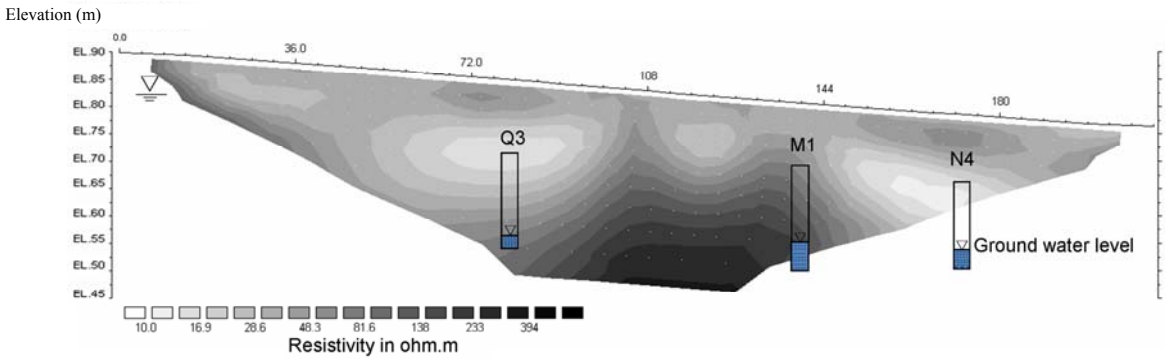

Fig. 8 Inverted resistivity cross-section for Line B along the passageway on the downstream shell

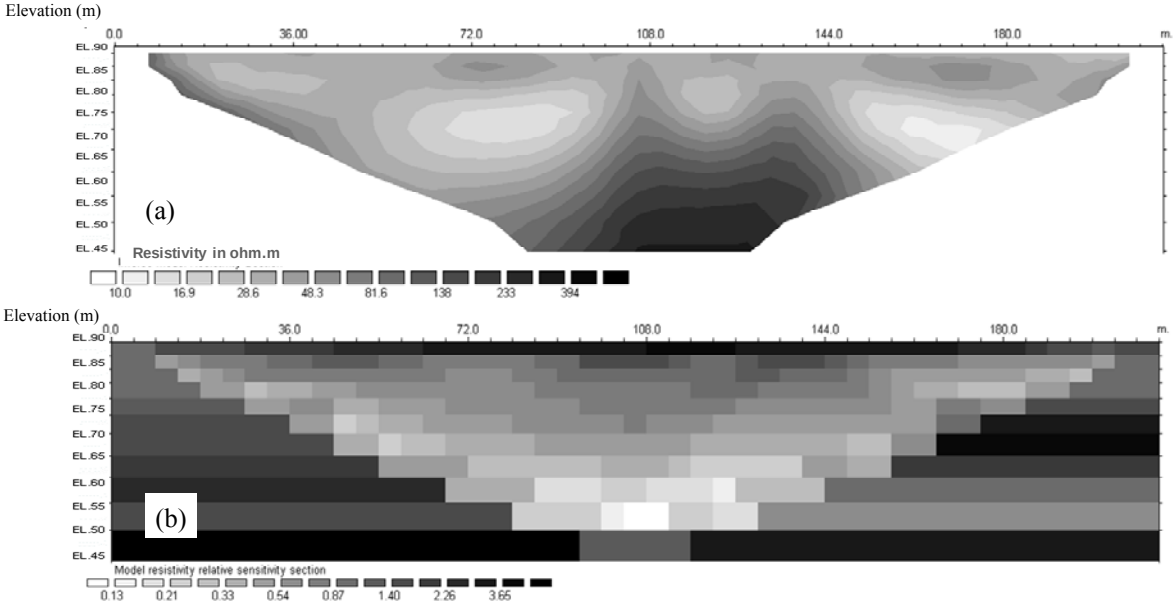

Fig. 9 (a) The resistivity image (before topography correction) for Line B; (b) the corresponding model blocks sensitivity

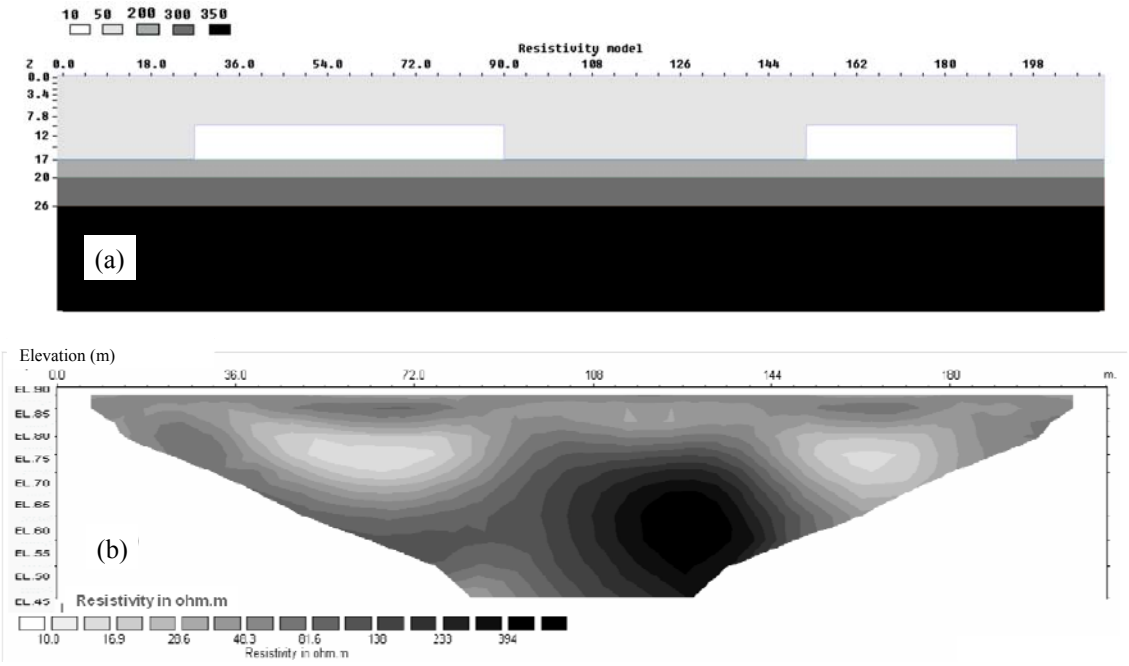

Fig. 10 (a) A simplified resistivity model for Line B; (b) inverted resistivity cross-section using synthetic data of the simplified model

simulating the field measurement. The inverted resistivity cross-section using the synthetic data is shown in Fig. 10(b). Great similarity can be found when it is compared with the result from actual field measurement (Fig. 9(a)). The uncertainty of the ERT inversion can be qualitatively comprehended by comparing the inverted cross-section (Fig. 10(b)) to the synthetic ground truth (Fig. 10(a)). Although the contour of the inverted resistivity model reveals apparent non-linear features, this is most likely artifacts resulted from poorly-resolved inversion. The results of Line A and Line B basically indicate two low resistivity zones in a more or less layered system. With this level of comprehension, over interpretation of ERT results can be avoided.

5.3 Analysis of Time-lapse Data

Single investigations presented above were used mainly to detect anomalous seepage in the dam. A single investigation typically is not able to give answers to crucial questions about the examined dam if carried out alone. But in combination with geotechnical data it may provide useful information as presented above. The time-lapse measurement adds another dimension (time) into the investigation and may provide additional information by studying the time-variation pattern. Line B is closest to the abnormal seepages. The ERT investigation at Line B was repeated a number of times on a monthly basis. No apparent anomaly with time was found by examining the inverted resistivity cross-sections at different times. Time-lapse inversion shows similar resistivity cross-section for each measurement. The results do not seem to provide additional information at a first glance. So a more quantitative interpretation in correlation with influencing factors (*i.e.*, reservoir water level and precipitation) is further analyzed. Figure 11 reveals the variation of average resistivity with time for one of the low resistivity zone and a relatively high resistivity area in between the two low resistivity zones. The reservoir level and two-week accumulated rainfall before each measurement are also shown to examine their correlations. The variation of reservoir level was not significant during the monitored period. For the low resistivity zone, the resistivity remain relatively constant irrespective to the precipitation variation. This further supports the speculation that the low resistivity zones are indications of perched groundwater and nearly saturated state. On the contrary, there is a significant correlation between resistivity and precipitation in the high resistivity area. This is a normal behavior of a homogeneous shell, in which the resistivity decreases with rainfall infiltration and increases as the vertical infiltration is eventually drained out by the horizontal drainage.

5.4 Integrated Interpretation of Abnormal Seepage Mechanism

The two low resistivity zones in Line B cross-section appear to spatially correlate with those two in Line A cross-section. Because the core inclines towards the upstream, the cross-section of Line A actually projects into the upper part of the shell. Line B extends from the top of the dam at the right abutment to the lower part of the shell at the left abutment. Possible paths for the anomalous seepage are depicted in Fig. 12 by combining the two cross-sections. These two possible pathways happen to correspond to the abnormal leakage spots 3 and 4 shown in Fig. 4, and further downstream to spots 1 and 2. The geophysical testing helps to reveal the underground pathways of the anomalous seepage. But interpretation for the possible mechanism requires integrating the geophysical results with geotechnical data. The dam was instrumented with several open standpipe piezometers. The dam cross-section near the abnormal leakage spots 2 and 4 is presented in Fig. 13 along with the results from ERT and piezometers. The phreatic line of the dam seepage is unexpectedly above the drainage layer at the lower part of the downstream shell as revealed by the hydraulic heads from Piezometer Q3 and Q4. This anomaly and the associated explanation require a separate investigation. The low resistivity zones and the possible pathways of the anomalous leakage at the downstream face are well above the phreatic line. This indicates that the abnormal leakage is not directly related to the steady-state seepage of the reservoir. According to the leakage monitoring, the amount of the abnormal leakage depend greatly on the precipitation. A possible explanation is that the perched low resistivity (wet) zones are due to rainfall infiltration trapped by some impermeable layers in the shell. The perched water finds its way out at the spot 4 and further downstream to the spot 2 with significantly less amount. The abnormal seepages found at the spot 3 and spot 1 seem to be in a similar situation.

6. CONCLUSIONS

The electrical resistivity tomography is increasingly used for seepage investigation. This study demonstrated the use of ERT and assessed the performance of ERT in the investigation of abnormal seepage at the Hsin-Shan earth dam, Taiwan. Results of three 2D ERT survey deployed on the left abutments, dam crest, and downstream shell reveal possible underground pathways of the anomalous seepage. But interpretation of resistivity value alone is challenging since variation of hydrophysical and geological conditions may co-exist. Periodic measurements were additionally collected on the downstream shell for time-lapse analyses. When the relation between resistivity and hydrological factor is quantitatively analyzed, time-lapse analyses can provide additional information on the possible mechanism of abnormal seepage. Integration of ERT exploration with time-lapse ERT measurements and geotechnical monitoring data was demonstrated to better understand the possible mechanism of the abnormal seepage.

To gain confidence and avoid over interpretation, it is desirable to carry out appraisal analysis of the ERT image. In-depth model appraisal is difficult. From engineers' point of view, forward model with educated guess based on ERT results seem to serve the purpose. For practical reasons, 2D resistivity surveying is often performed on the dam crest or downstream slope in longitudinal direction as also is the case in this study. Along these survey lines, 2D assumption is violated due to the influence of geometry and material properties from zoning of the dam body. Possible 3D effect on the 2D inversion is under investigation.

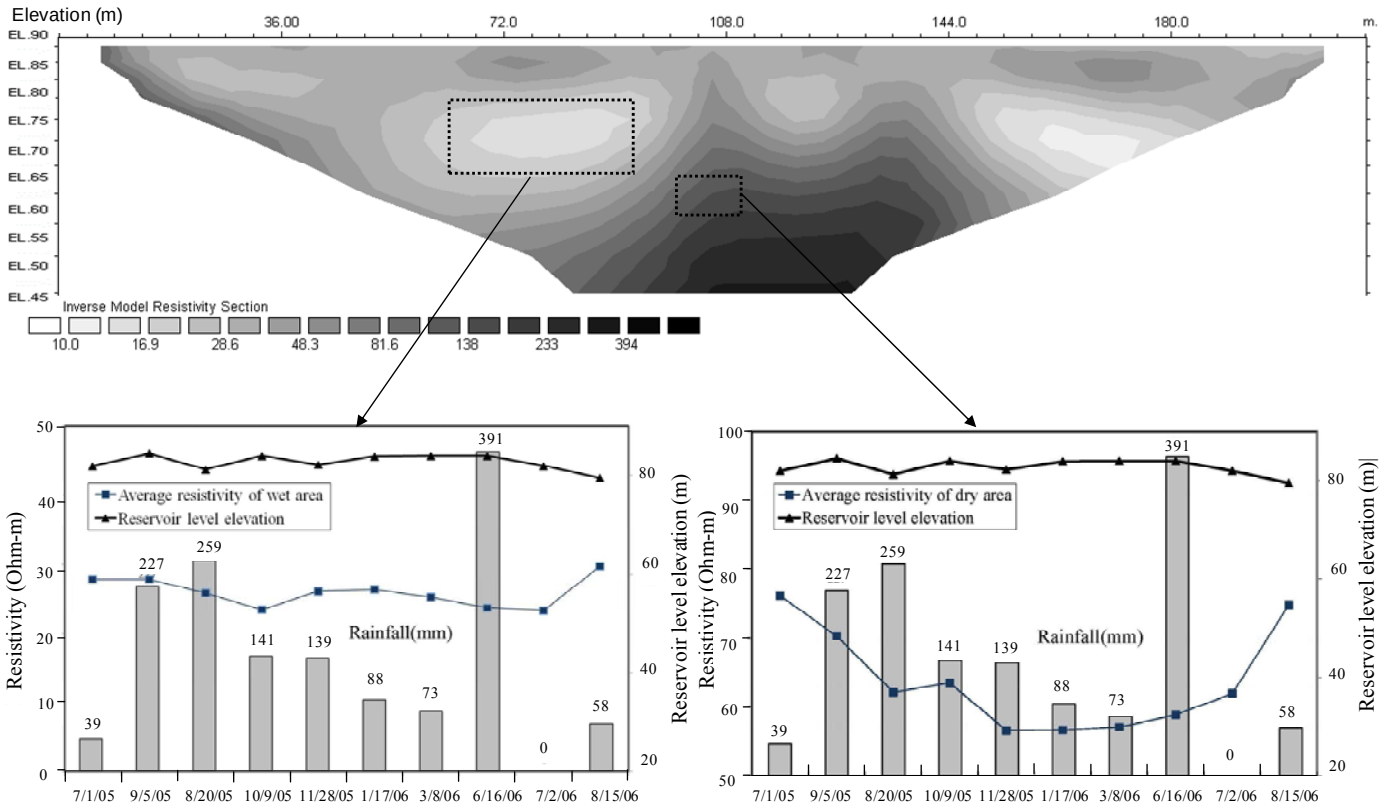

Fig. 11 Time-lapse resistivity in relation with reservoir water level and precipitation in the low resistivity (left) and high resistivity (right) zone

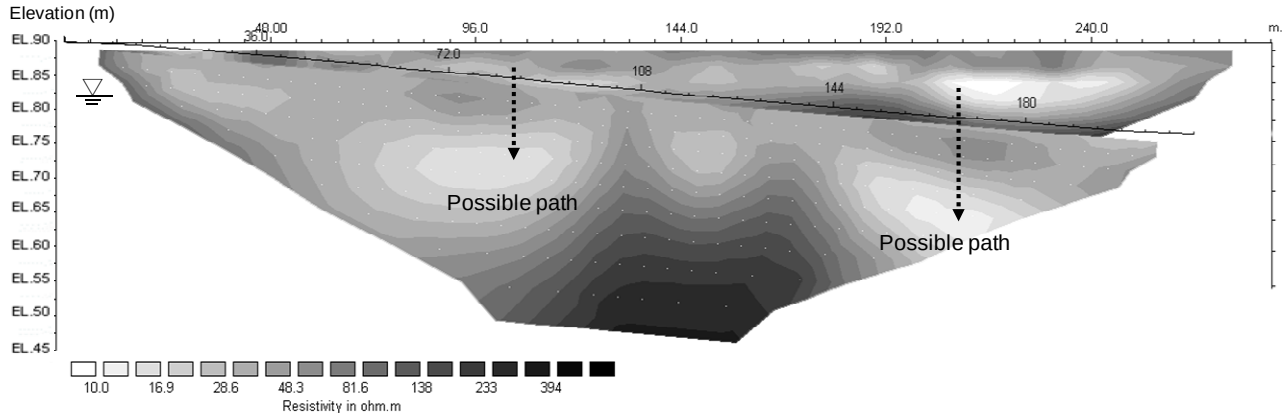

Fig. 12 Combined representation of results from Line A and Line B

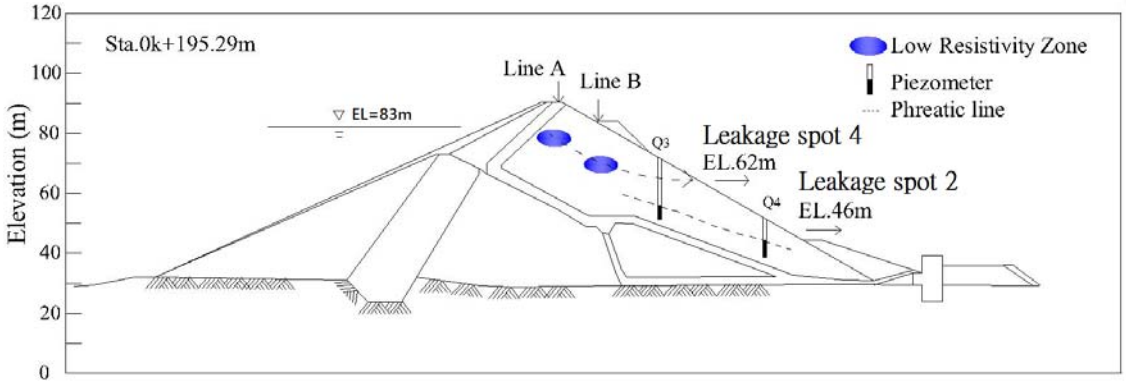

Fig. 13 The low resistivity zones from ERT and hydraulic heads from piezomters on the dam cross-section near abnormal leakage spots 2 (EL. 46 m) and 4 (EL. 62 m)

REFERENCES

Abuzeid, N. (1994). "Investigation of channel seepage areas at the existing Kaffrein Dam site (Jordan) using electrical-resistivity measurements." *Journal of Applied Geophysics*, **32**, 163–175.

Barker, R. and Moore, J. (1998). "The application of time-lapse electrical tomography in groundwater studies." *Leading Edge*, **17**, 1454–1458.

Bentley, L. R. and Gharibi, M. (2004). "Two- and three-dimensional electrical resistivity imaging at a heterogeneous remediation site." *Geophysics*, **69**, 674–680.

CGS (Central Geological Survey) (1998). *Explanatory Text of the Geologic Map of Taipei (1:50,000)*, Ministry of Economic Affairs, Taipei, Taiwan (in Chinese).

Cho, I. K. and Yeom, J. Y. (2007). "Crossline resistivity tomography for the delineation of anomalous seepage pathways in an embankment dam." *Geophysics*, **72**, 31–38.

Dahlin, T. and Leroux, V. (2006). "Time-lapse resistivity investigations for imaging saltwater transport in glaciofluvial deposits." *Environmental Geology*, **49**, 347–358.

Dahlin, T. and Zhou, B. (2004). "A numerical comparison of 2D resistivity imaging with 10 electrode arrays." *Geophysical Prospecting*, **52**, 379–398.

Friedel, S. (2003). "Resolution, stability and efficiency of resistivity tomography estimated from a generalized inverse approach." *Geophysics Journal International*, **153**, 305–316.

Geotomo Software (2002). *RES2DMOD Ver. 3.01*, Rapid 2-D resistivity forward modeling using the finite-difference and finite-element methods, available at www.geoelectrical.com.

Geotomo Software (2007). *RES2DINV Ver. 3.56*, Rapid 2-D resistivity and IP inversion using the least-squares method, available at www.geoelectrical.com.

Griffiths, D. H., Turnbull, J., and Olayinka, A. I. (1990). "Two-dimensional resisitivity mapping with a computer-controlled array." *First Break*, **8**, 121–129.

Johansson, S. and Dahlin, T. (1996). "Seepage monitoring in an earth embankment dam by repeated resistivity measurements." *European Journal of Engineering and Environmental Geophysics*, **1**, 229–247.

Karastathis, V. K., Karmis, P. N., Drakatos, G., and Stavrakakis, G. (2002). "Geophysical methods contributing to the testing of concrete dams, application at the Marathon Dam." *Journal of Applied Geophysics*, **50**, 247–260.

Kim, J. H., Yi, M. J., Song, Y., Seol, S. J., and Kim, K. S. (2007). "Application of geophysical methods to the safety analysis of an earth dam." *Journal of Environmental and Engineering Geophysics*, **12**, 221–235.

Lee, J. Y., Choi, Y. K., Kim, H. S., and Yun, S. T. (2005). "Hydrologic characteristics of a large rockfill dam: Implications for water leakage." *Engineering Geology*, **80**, 43–59.

Lim, H. D., Kim, K. S., Kim, J. H., Kwon, H. S., and Oh, B. H. (2004). "Leakage detection of earth dam using geophysical methods." *Proceedings of the 72th Annual Meeting of International Commission on Large Dams (ICOLD)*, 212–224.

Lin, C. P., Pan, Y. W., and Liao, J. J. (2005). *Review of Monitoring Problems and Application of Non-Destruction Testing Methods for Evaluation Dam Performance*, Water Resources Agency Research Report MOEAWRA0940206 (in Chinese). Loke, M. H. (2001). "Constrained time-lapse resistivity imaging inversion." *Proceedings of the 14th Annual Symposium on the Application of Geophysics to Engineering and Environmental Problems*, 34.

Malkawi, A. I. H. and Al-Sheriadeh, M. (2000). "Evaluation and rehabilitation of Dam seepage problems. A case study: Kafrein dam." *Engineering Geology*, **56**, 335–345.

Nguyen, F., Kemna, A., Antonsson, A., Engesgaard, P., Kuras, O, Ogilvy, R., Gisbert, J., Jorreto, S., and Pulido-Bosch, A. (2009). "Characterization of seawater intrusion using 2D electrical imaging." *Near Surface Geophysics*, **7**, 377–390.

Oh, Y. C., Jeong, H. S., Lee, Y. K., and Shon, H. (2003). "Safety evaluation of rock-fill dam by seismic (MASW) and resistivity method." *Proceedings of the 16th Annual Symposium on the Application of Geophysics to Engineering and Environmental Problems*, 1377–1386.

Okko, O., Hassinen, P., and Korkealaakso, J. (1994). Location of Leakage Paths Below Earth Dams by Geophysical Techniques: Proceedings of the 13th International Conference on Soil Mechanics and Foundation Engineering (ICSMFE), 1349–1352, New Delhi.

Oldenborger, G. A. and Routh, P. S. (2009). 'The point-spread function measure of resolution for the 3D electrical resistivity experiment." *Geophysical Journal International*, **176**, 405–414.

Oldenburg, D. and Li, Y. (1999). "Estimating the depth of investigation in DC resistivity and IP surveys." *Geophysics*, **64**, 403–416.

Panthulu, T. V., Krishnaiah, C., and Shirke, J. M. (2001). "Detection of seepage paths in earth dams using self potential and electrical resistivity methods." *Engineering Geology*, **59**, 281–295.

Song, S. H., Song, Y., and Kwon, B. D. (2005). "Application of hydrogeological and geophysical methods to delineate leakage pathways in an earth fill dam." *Exploration Geophysics*, **36**, 92–96.

Sjödahl, P., Dahlin, T., and Johansson, S. (2005). "Using resistivity measurements for dam safety evaluation at Enemossen Tailings Dam in Southern Sweden." *Environmental Geology*, **49**, 267–273.

Sjödahl, P., Zhou, B., and Dahlin, T. (2006). "2.5D resistivity modeling of embankment dams to assess influence from geometry and material properties." *Geophysics*, **71**, 107–114.

Sjödahl, P., Dahlin, T., and Johansson, S. (2010). "Using the resistivity method for leakage detection in a blind test at the Røssvatn embankment dam test facility in Norway." *Bulletin of Engineering Geology and the Environment*, **69**, 643–658.

TWC (Taiwan Water Corporation) (2001). *Report of the Second Safety Evaluation of Hsin-shan Reservoir*. Taiwan Water Corporation, Taichung, Taiwan (in Chinese).

Turkmen, S., Öeguler, E., Taga, H., and Karaogullarindan, T. (2002). "Detection and evaluation of horizontal fractures in earth dams using the selfpotential method." *Engineering Geology*, **63**, 247–257.

Voronkov, O. K., Kagan, A. A., Krivonogova, N. F., Glagovsky, V. B., and Prokopovich, V. S. (2004). "Geophysical methods and identification of embankment dam parameters." *Proceedings of the 2nd International Conference on Geotechnical and Geophysical Site Characterization*, 593–599.